2012

Dual-Mode Wicking Structures for Enhanced Evaporative Heat Transfer

Shankar Krishnan
ward.tegrotenhuis@pnnl.gov

Ward E. TeGrotenhuis

Dual-Mode Wicking Structures for Enhanced Evaporative Heat Transfer

Shankar KRISHNAN[1,2]* and Ward TEGROTENHUIS [1,2]
[1]Microproducts Breakthrough Institute,
Corvallis, Oregon, USA
(541)713-1206, shankar.krishnan@pnnl.gov

[2] Pacific Northwest National Laboratory, Thermal and Reaction Systems,
Richland, Washington, USA

* Corresponding Author

ABSTRACT

This paper reports on conceptual design and thermo-fluid characteristics of two-phase flow devices enabled by dual-mode wicks. In dual-mode wicking structures, liquid and vapor flow paths are integrated on the same plane and segregated flow of the two-phases is achieved by having networks of pores of multiple length-scales. When a mixture of a gas and a liquid flow through this media and the wick material wets the liquid, then the liquid will preferentially segregate to and flow through the mode with the smaller effective pore size. The gas will flow through the paths with the larger effective pore size. These wicks, further, have advantages in phase change heat exchange where the liquid can fill the entire channel. The interwoven liquid and vapor paths facilitate phase segregation and suppress or delay dry out of heated surfaces. Experimental results are presented showing heat transfer coefficients exceeding 25,000 W/m^2K. Other characteristics demonstrated include reduced pressure drop and pressure fluctuations, and lower superheat requirements when compared to empty channels. A theoretical basis for enhanced heat transfer is presented, and merits of employing the technology in energy conversion applications are discussed.

1. INTRODUCTION

Processing gases and liquids together in microchannels having at least one dimension less than 1 mm has unique advantages for heat and mass transfer. Many investigators have proposed an assortment of microchannel based technologies and have studied multiple applications in science and engineering (Stone and Kim, 2001) and Stone et al, 2004). Liquid-vapor phase change heat transfer is a critical process in many energy conversion systems, including vapor compression and absorption cycle cooling, and for power cycles. Two-phase flow and heat transfer in microchannels have also been studied by many investigators for applications in electronics cooling. A thorough review of all the literature is beyond the scope of this paper.

One approach for managing the two phases is to use porous structures as wicks within microchannels to segregate the liquid phase from the gas/vapor phase. Gas-liquid processing is accomplished by providing a gas flow path and inducing flow of the liquid phase through the wick under an induced pressure gradient. These microwick technologies enable a variety of unit operations including phase separation, partial condensation, absorption, desorption, and distillation as discussed in TeGrotenhuis and Stenkamp (2005). The objective here is to extend the application of microwick technologies to enable energy efficient evaporators in energy conversion systems. Wicking structures assisted evaporation and thermal transport is popularly employed in heat pipes and its variants, Faghri (1995). Two-phase flows in capillary structures have also been studied by some investigators in the past, Wang and Peterson (2010) and Kawashima et al (1999). In this paper, we investigate two-phase evaporative flows in micro-scale capillary structures. We report evaporative heat transfer and fluid flow performance characteristics on dual-mode (characterized by multiple length and time scales) wicking structures. We compare our results against a simple empty-channel of the same dimensions in order to assess the advantages of microwick evaporators.

2. DUAL-MODE WICKS

Dual-mode wicks refer to a class of porous structures that have multiple, distinct effective pore sizes, such as the structure made from Dexmet expanded metal foils shown in left image of Figure 1. The spaces between adjacent wires correspond to one pore length-scale while the larger diamond-shaped openings correspond to a second pore length-scale. When one observes a capillary rise experiment, liquid imbibes into the smaller gaps between the wires more rapidly and to a higher level than into the larger openings. The analogy is a bundle of capillary tubes of differing diameter. The smallest tubes have the highest capillary driving force and will fill first. When the end is dipped in a wetting fluid, the smallest tubes fill faster and to a higher level while the mode corresponding to the largest diameter tube fills slowest and is 'volume filling'.

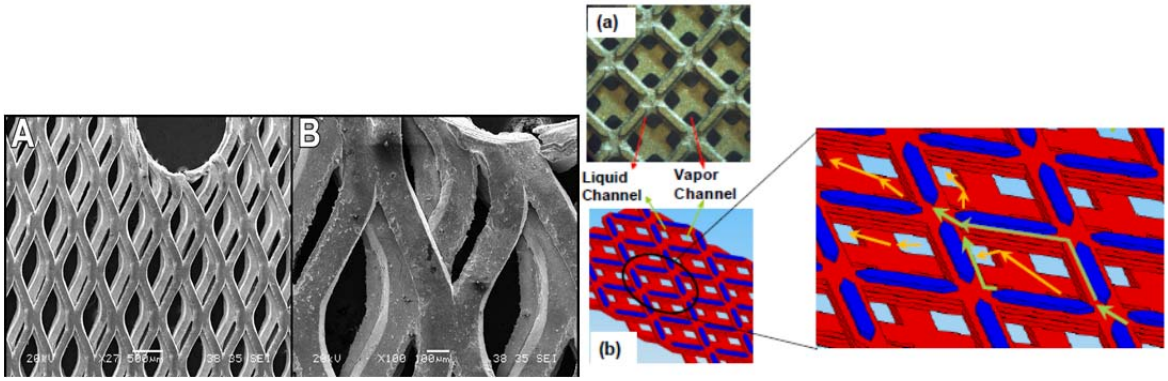

Figure 1. Examples of dual-mode wicks, including a 2-layer Dexmet expanded metal foil wick (A and B) and a second constructed of photo chemically machined (PCM) layers (a) with a schematic showing flow paths (b).

2.1 Capillary Rise Experiments

For a wick with one effective pore size, the mass uptake curve can be fit using the equation

$$q = \frac{K}{\mu L}\left(\frac{2\sigma\cos(\theta)}{r_p} - \rho g L\right) \tag{1}$$

which is Darcy's Law combined with a pressure balance between capillary pressure from the Young-Laplace equation and hydrostatic head, where q is the velocity, K is permeability, μ is fluid viscosity, L is the liquid height, σ is the liquid surface tension, θ is the contact angle between the liquid and the material, r_p is the effective pore radius, ρ is the liquid density, and g is the gravitational constant. Figure 2 illustrates the poor fit of Equation (1) to capillary rise data for a dual-mode wick. However, if a second length-scale is admitted with different parameters for K, $L(t)$, and r_p, then the data can be more accurately fit, as shown by the second curve in Figure 2. This provides quantitative evidence in addition to qualitative observations for the dual-mode behavior.

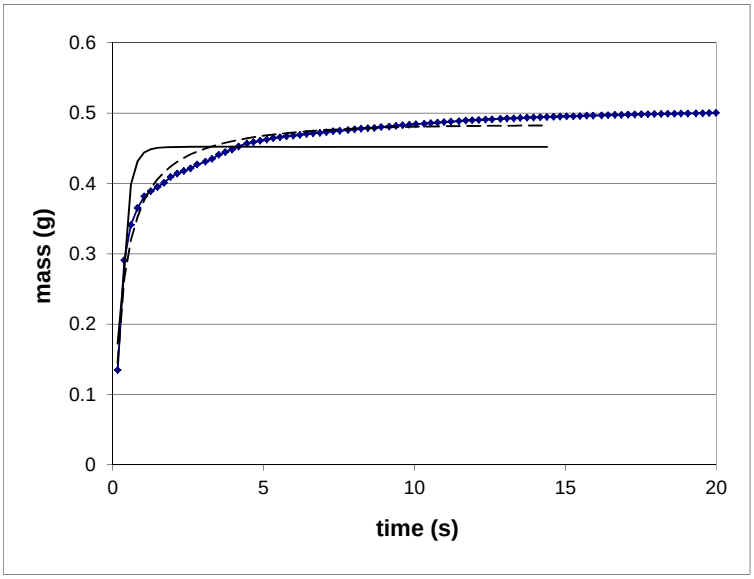

Figure 2. Mass uptake data (♦) for a capillary rise experiment with ethylene glycol in a 3-layer wick made of 4Al7-050F Delker expanded metal screens. Least squares curve fit (—) of the data to the single-mode capillary rise equation and to the dual-mode capillary rise equation (- -).

2.2 Phase Change Heat Transfer

The objective is to take advantage of the unique hydrodynamic properties of dual-mode wicks for gas-liquid processing. When a mixture of a gas and a liquid flow through this media and the liquid wets the wick material, liquid will preferentially segregate to the smaller pore sizes and gas will flow through the larger effective pores to minimize pressure drop. Whereas heat pipes typically contain a wick for liquid flow and a separate plenum for vapor flow, the ability for dual-mode wicks to accommodate separate liquid and vapor flow paths creates the opportunity for 'volume filling' wicks, as one example. Additionally, segregating gas and liquid into separate flow paths suppresses pressure fluctuations and liquid carryover that typically occurs in two-phase flow.

Furthermore, advantages are anticipated for phase change heat transfer, which is the primary subject of this paper. When a dual-mode wick is in thermal contact with a primary heat transfer surface, the wick provides secondary heat transfer area and improves heat distribution into the channel, as well as providing significantly higher surface area and nucleation sites to enhance boiling. Dry out is delayed by the capillary flow which distributes liquid and by flow segregation which avoids vapor trapping. Gas phase convective heat transfer is enhanced by the small hydraulic diameter and tortuosity of the vapor channels, while the total vapor phase flow area created by the large number of parallel vapor channels precludes excessive pressure drops.

3. PHASE CHANGE EXPERIMENTS

3.1 Test Device

In order to explore the potential for enhancing phase change heat transfer, a well-define dual-mode wick geometry was created from the photo-chemically machined (PCM) layers shown in Figure 1(a), which were made from 0.102 mm thick 316 stainless-steel shims. The square openings are 0.5 mm on a side. When two layers are stacked with the holes aligned, the gaps between the wires form capillary channels that are approximately 0.05 mm wide and are continuous from one edge of the wick to the other. Continuous, tortuous vapor channels are created by offsetting adjacent layers as shown in Figure 1(b). The liquid and vapor flow paths are illustrated in Figure 1(b). A test device was constructed by stacking 8 layers in an enclosure. The total flow cross-section had dimensions of 0.8 mm by 3.8 cm and the total flow length was 10.2 cm.

3.2 Experimental Set-up and Analysis

Figure 3 shows a schematic of the phase change experimental set-up used to acquire boiling heat transfer performance of the dual-mode test device as well as an empty channel with the same internal dimensions for comparison. The device is oriented horizontally with gravity acting in the 0.8 mm dimension and is submerged in a

HAAKE D8 heated bath containing propylene glycol that was maintained at a set point within ± 0.25°C. Filtered, de-ionized water is metered to the device using a peristaltic pump and a McMillan Micro flow sensor. Upon passing through the test device, the flow exits to a weighed container. Terminal temperatures and pressure difference across the device are measured using calibrated Omega T-type thermocouples (standard error ± 1.0 °C) and Sensotec differential pressure transducer, respectively.

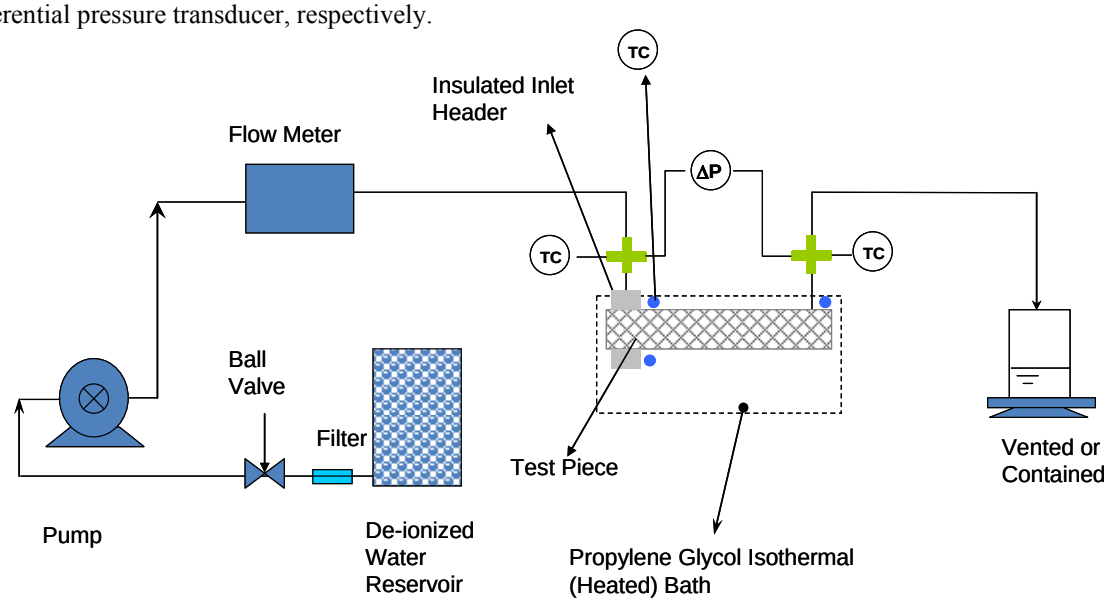

Figure 3. Schematic of phase change heat transfer experimental set-up.

Total heat transfer rate was calculated by an enthalpy balance using the mass flow and inlet and outlet temperatures and pressures. Exit vapor quality was determined from the liquid effluent flow rate, which was obtained from the weight accumulation in the container.

The heat transfer analysis assumes the device wall-temperature is the same as the bath set-point and that the wall resistance is negligible, so the heat transfer resistance is dominated by the heat transfer coefficient within the test device channel. The liquid feed was sub-cooled and the effluent was superheated in many cases, so single-phase heat transfer coefficients were needed to determine the subcooled, two-phase, and superheat lengths within the device using the same techniques as Bertsch et al. (2008). The same experimental system was used to obtain single-phase heat transfer coefficients for both liquid and gas. The single phase heat transfer coefficient for liquid water is given by the correlation

$$\mathrm{Nu}_{\sqrt{A}} = 0.14\,\mathrm{Re}^{0.67} \tag{2}$$

and for superheated steam is given by

$$\mathrm{Nu}_{\sqrt{A}} = 0.7\,\mathrm{Re}^{0.67} \tag{3}$$

The experimental data had a R^2 value of 99.4 % for the Reynolds number range of 27-300 encountered in testing. The sub-cool and superheat duties are calculated from the inlet and outlet conditions, respectively, which are subtracted from the total to obtain the two-phase duty. The lengths of sub-cool and superheat sections are obtained from their duties, heat transfer coefficients, and log-mean temperature difference with the constant wall temperature. The remaining device length is used as the two-phase transfer length to obtain the primary two-phase heat transfer area. Finally, the two-phase heat transfer coefficient is obtained from the equation

$$h_{tp} = \frac{q_{tp}}{T_{bath} - T_{sat}} \tag{4}$$

where q_{tp} is the two-phase heat transfer flux, T_{bath} is the bath temperature, and T_{sat} is the water saturation temperature.

4. EXPERIMENTAL RESULTS

4.1 Dual-Mode Results

A series of experiments were performed at different mass flow rates and different bath temperatures at atmospheric pressure within the device, so saturation temperature was 100°C. Figure 4 shows plots of bath temperature versus fluid exit temperature for the dual-mode wick evaporator. At all three flow rates, onset of boiling occurs very close to 100°C bath temperature. In the two-phase region where the measured temperature alternates between saturation and superheat temperatures, only the saturation temperature is plotted in Figure 4. At the lowest flow rate at a mass flux of 15.7 kg/m^{2}s, very little driving force is needed to fully vaporize the water, and the exit temperature tracks the bath temperature with only 15°C driving force. At the intermediate flow, the required driving force increases to about 40°C, and at the highest flow rate, the water is not fully vaporized with 50°C driving force. The estimated capillary pumping capacity of the wick corresponds to a mass flux of 85 kg/m^{2}s.

The two-phase heat transfer coefficient and pressure drop are plotted in Figures 5 and 6 as a function of non-dimensional groups for the same three water flow rates. Heat transfer coefficients as high as 25,000 W/m^2·K were obtained with water, which is over 3 times higher than values typically obtained with brazed-plate heat exchangers using R-410a refrigerant (Han et al., 2003, Hsieh et al. 2002).

A dimensional analysis is performed to try to elucidate the physical processes occurring in two-phase heat transfer within the dual-mode wick. If capillarity is a controlling mechanism, as desired, then scaling with the liquid channel effective pore diameter, d, and surface tension, σ, should be valid. As expected, gravity is not important when the device is oriented horizontally, which is confirmed by the Bond number ($=\rho g d_h^2/\sigma$), which is on the order of 10^{-5}, where d_h is the liquid channel hydraulic diameter and ρ is liquid density. Therefore, for Bo << 1, the Suratman number ($=\rho\sigma d/\mu^2$) is the relevant group for scaling inertial forces in capillary flows, which is in the range of 2-4x10^5 for water in the range of 20-100°C. Jayawardane et al (1997) performed extensive investigations of capillary flow in the viscous dominated regime (Su=10^3-10^5). Whereas the boiling behavior observed in tubes involves transitions between bubbly flow, churn, slug, annular or film, and mist flow, the expectation is that flow behavior in dual-mode wick in the two-phase boiling region is capillary driven. The Jakob number (Ja= $C_p(T_{bath}-T_{sat})/h_{fg}$) is important for discerning the relative importance of sensible versus latent heat transfer. Other relevant groups for heat and mass transfer are the Reynolds number (*Re*), Prandtl number (*Pr*), and Peclet number (*Pe*).

The simplified physical model used for scaling is heat conduction through a liquid film of uniform thickness δ over the entire two-phase heat transfer area. A heat and mass balance over the length of the two-phase region, L_{tp}, results in

$$k_l \frac{\left(T_{bath} - T_{sat}\right)}{\delta} L_{tp} = h_{fg}\, \rho_l V_l\, \delta \tag{5}$$

where k_l is liquid thermal conductivity, h_{fg} is the heat of vaporization, ρ_l is liquid density, and V_l is liquid velocity at the start of the two-phase region which goes to zero over the two-phase length. If the two-phase heat transfer coefficient is dominated by heat conduction through the film, the Nusselt number can be estimated by

$$Nu \sim \frac{h_{tp} k_l}{\delta} \sim \left(\frac{Pe}{Ja}\right)^{0.5} \left(\frac{d}{L_{tp}}\right)^{0.5} \tag{6}$$

using Equation (5). Using this scaling to plot two-phase heat transfer coefficients produces straight lines, as shown in Figure 5, that coincide at low Pe number and deviate at higher Pe. This supports the starting assumption that two-phase heat transfer is dominated by thin film conduction in the dual-mode wick. Furthermore, if the film thickness is equal to the liquid channel effective pore diameter, then the data would fall on the theoretical line included in Figure 5. The proximity of the line to the data and the consistent slope indicate the film thickness is on the same order. The offset between the data and the line is likely due to neglected thermal resistances, in particular, resistance due to conduction from the outer wall through the wick to the thin films.

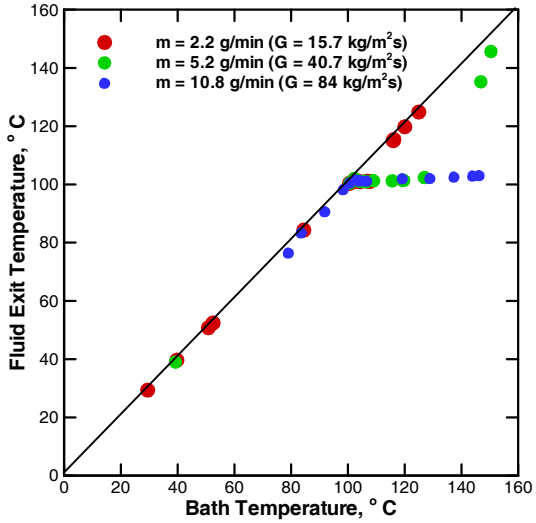

Figure 4. Fluid exit temperature versus bath temperature at three different water flow rates.

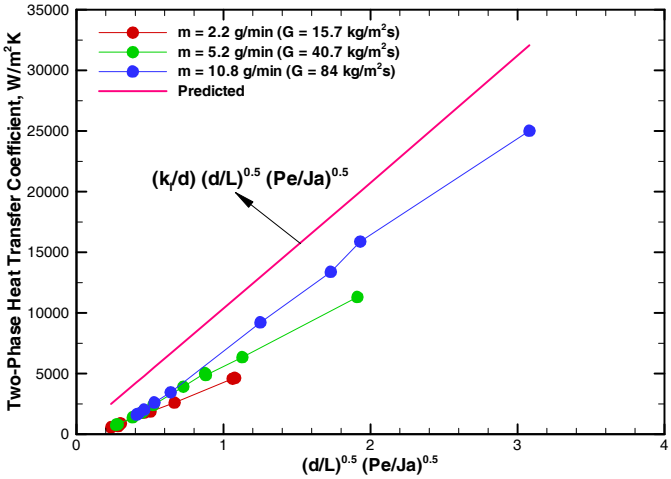

Figure 5. Two-phase heat transfer coefficient as a function of modified Peclet number.

4.1 Comparison to Empty Channel

Figure 6 shows the comparison between empty channels and dual-mode wicks of the same total internal dimensions. The improvement with the dual-mode wick is seen in Figure 6 as the bath temperature rises above 110°C. With greater than 10°C driving force, the dual-mode wick device fully vaporizes the water, while the empty channel continues to show outlet temperatures oscillating between saturated liquid and superheated vapor. Even at 20°C temperature driving force, the empty channel shows 2-phase flow at the outlet. The empty channel oriented horizontally did not produce a consistent superheated steam at any of the water flows and bath temperatures that were tried. The illustrates that not only can dual-mode wicks improve the boiling heat transfer coefficient, but 100% quality vapor can be stably produced at lower superheat.

Pressure drop measurements from the differential pressure transducer show larger pressure oscillations with the empty channel than with the dual-mode wick device, as shown in Figure 7. The dual-mode wick device does show an increase in pressure drop of about 0.3 psi at 15.7 g/s.m^2 mass flux. Similar behavior was observed at the higher flow rate of 5.2 g/min. Pressure oscillations in the empty channels are understood to be caused by slugging due to varying vaporization rates and periodic dry out. The capillary flow paths for the liquid in combination with separate flow paths for the vapor creates more consistent flow dynamics, delays dry out effects, and provides much more stable pressure performance. This is likely to be most important in closed-loop systems where pressure fluctuations can propagate and induce unstable feedback mechanisms.

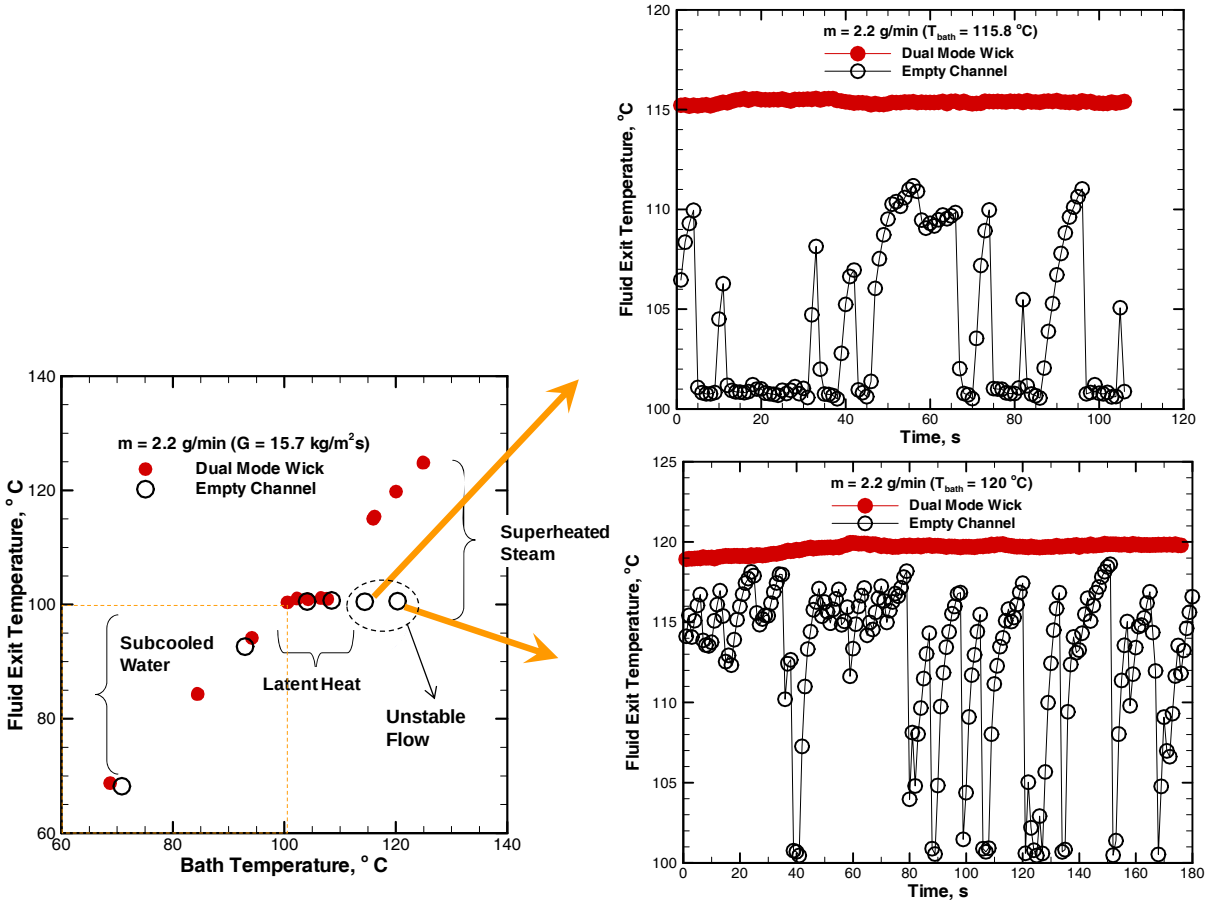

Figure 6: Comparison of minimum fluid exit temperature versus bath temperature between dual-mode wick and empty channel evaporator at a mass flux of 15.7 g/s.m^2, as well as time traces showing fluctuations.

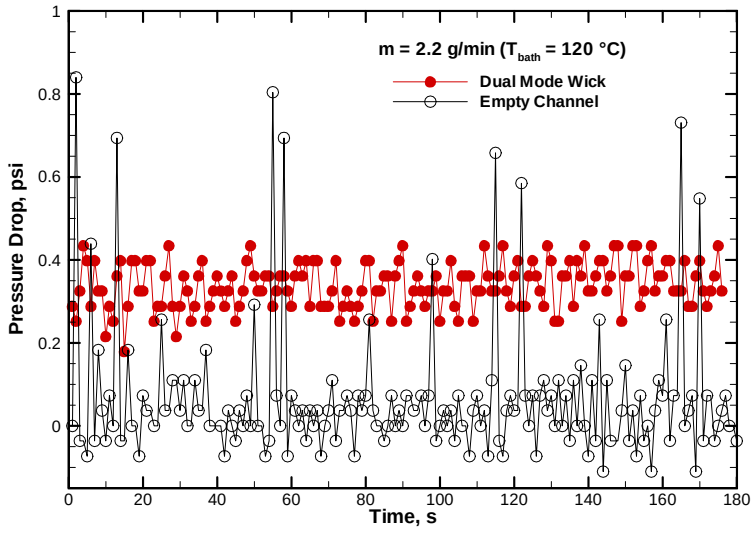

(b)

Figure 7: Comparison of pressure drop between dual-mode wick and empty channel evaporator at a mass flux of 15.7 g/s.m^2 and 120°C bath temperature.

5. CONCLUSIONS

This paper described unique structures for processing gas-liquid mixtures and reported on thermo-fluid characteristics of a dual-mode wick device. A two-phase heat transfer coefficient exceeding 25,000 W/m^{2}K was obtained with a dual-mode wick device. Scaling calculations were presented supporting a thin film heat transfer model with a film thickness comparable to the liquid channel effective pore diameter. In comparison to an empty channel device, the dual-mode wick device enabled:

- stable operation (without pressure and temperature oscillations) and generally self-regulating due to capillary action
- enhanced heat transfer and hence reduced superheat requirement for evaporative heat exchanger applications, and
- complete vaporization of liquid to vapor at lower superheat.

REFERENCES

Bertsch et al, 2008, Refrigerant flow boiling heat transfer in parallel microchannels as a function of local vapor quality, International Journal of Heat and Mass Transfer, Vol. 51, pp. 4775-4787.

Faghri, A., 1995, Heat Pipe Science And Technology, Taylor and Francis.

Han, D-H, K-J Lee, and Y-H Kim, "Experiments on the characteristics of evaporation of R410A in brazed plate heat exchangers with different geometric configuration", Appl. Thermal Eng. **23** (2003) 1209-1225.

Hsieh, Y.Y. and T.F. Lin, "Saturated flow boiling heat transfer and pressure drop of refrigerant R-410A in a vertical plate heat exchanger", Int. J. Heat and Mass Transfer, **45** (2002) 1033-1044.

Jayawardena, S., et al., 1997,Flow Pattern Transition Maps for Microgravity Two-Phase Flows, AIChE J., Vol. 43, pp. 1637–1640.

Kawashima, H, 1999, Similarity solutions for pressure-driven boiling flows in capillary porous media, International Communications Heat and Mass Transfer, Vol. 26, pp.319-327.

Krishnan, S., and TeGrotenhuis, W.E., Dual-Mode Wicking Structures for Enhanced Evaporative Heat Transfer, Article in Preparation.

Stone H. A., and Kim, S., 2001, Microfluidics: Basic Issues, Applications, and Challenges, AIChE Journal, Vol. 47, pp. 1250-1254.

Stone et al, 2004, Engineering Flows in Small Devices: Microfluidics Toward a Lab-on-a-Chip, Annual Review of Fluid Mechanics, Vol. 36, pp. 381-411.

TeGrotenhuis, W. E., and Stenkamp, V. S., 2005, Gas-Liquid Processing in Microchannels, Microreactor Technology and Process Intensification (Y. Wang and J. D. Holladay eds.), ACS Symposium Series 914, Washington, DC, pp. 360-377.

Wang, H., and Peterson, R., 2007, Flow Boiling Enhancement in Microchannels with Diffusion Bonded Wire Mesh," Proceedings of ASME/JSME Summer Heat Transfer Conference, Paper # HT2007-32119.

ACKNOWLEDGEMENTThe authors would like to acknowledge the financial support provided by US Army Communications-Electronics Research, Development, and Engineering Center (CERDEC) through the Tactical Energy System program W909MY-10-C-0073.